MEDS Chinese Medicine (2022)
Clausius Scientific Press, Canada

DOI: 10.23977/medcm.2022.040502
ISSN 2616-1753 Vol. 4 Num. 5

To Explore the Mechanism of Jinshui Tinling Decoction in the Treatment of Malignant Pleural Effusion Based on Network Pharmacology and Molecular Docking Technology

Baogang Yang[1,a], Chenguang Yang[2,b,*], Jiao Gou[2,c]

[1]Shaanxi University of Traditional Chinese Medicine, Xianyang, 712046, China
[2]Shaanxi Hospital of Traditional Chinese Medicine, Xi'an, 710000, China
[a]youaremysmile153@163.com, [b]470999091@qq.com, [c]sunnyxjdt@qq.com
**Corresponding author*

Keywords: Malignant pleural effusion, jingshui Tinling decoction, network pharmacology, β-sitosterol, AKT1, molecular docking

Abstract: **Objective** To explore the mechanism of action of Jingshui Tinling decoction (JSTLD) treating Malignant pleural effusion (MPE) by using network pharmacology and molecular docking technology. **Methods** The active components of JSTLD were screened by TCMSP database and UniProt database. The targets related to MPE were screened by Genecards database and OMIM database, and the intersection targets of active components and disease-related targets were obtained, namely, the targets of JSTLD in the treatment of MPE. Cytoscape 3.8.2 software was used to construct the "drug-active ingredient-target" network, and the core active components in the network were analyzed. The intersection targets were imported into STRING database for protein interaction (PPI) network analysis, and core targets were screened out. GO and KEGG enrichment analysis of core targets were carried out. Autodock vina 1.1.2 software was used for molecular docking of core components and targets. **Results** Network pharmacological prediction showed that there were 153 active components of JSTLD, 8463 corresponding target genes, 1539 MPE disease-related targets, and 106 intersection targets. The core active components such as quercetin, β-sitosterol, kaempferol and stigmasterol were obtained. AKT1, TP53, IL1B, CASP3, JUN, EGFR and other core targets; A total of 233 signaling pathways were screened, and the key pathways included cancer pathways. The molecular docking results are good. **Conclusion** JSTLD may act on AKT1, TP53, IL1B, CASP3, JUN, EGFR and other targets, and inhibit MPE through the cancer pathway and other related pathways.

1. Introduction

Malignant pleural effusion (MPE) is caused by the invasion of the pleura by malignant tumors, which are often directly invaded or metastasized to the pleura by lung cancer, breast cancer, malignant pleural mesothelioma and lymphoma [1]. The appearance of MPE not only causes dyspnea, which seriously affects the quality of life of patients, but also often indicates that the survival of patients is

very limited [2]. At present, the treatment of MPE is mainly based on local treatment such as chest tube drainage and talc internal pleural fixation. According to the different diseases, whether to give chemotherapy, targeting, immune and other systemic treatment. Chest tube drainage and/or talc pleurodesis are recommended by US and European guidelines [2,3], but local treatment only improves dyspnea symptoms and does not prevent MPE production. Although the systemic treatment of MPE targets the primary disease, its efficacy is not ideal. Chemotherapy is only effective for some MPE caused by tumors sensitive to chemotherapy drugs, and the efficacy of targeted and immunotherapy still needs to be verified by large-scale RCT studies [4]. It is still an urgent clinical problem to find a therapeutic method with better efficacy and less adverse reactions. Jinshui Tinling Decoction (JSTLD) was developed by Professor Chenguang Yang of the Oncology Department of Shaanxi Provincial Hospital of Traditional Chinese Medicine based on the "Mingmen " of traditional Chinese medicine and clinical experience [5], and has been awarded the national invention patent [6]. Retrospective clinical research results show that JSTLD can effectively control MPE and prolong the survival of patients [7]. This study intends to explore the effective active ingredients, core targets and potential mechanism of JSTLD in the treatment of MPE by using network pharmacology and molecular docking technology, in order to provide scientific basis for clinical and experimental research.

2. Materials and Methods

2.1. Screening of active Ingredients and Targets of JSTLD

In this study, through the Traditional Chinese Medicine Systematic Pharmacology Database and Analysis Platform (TCMSP, Traditional Chinese Medicine Systems Pharmacology Database and Analysis Platform, https://tcmspw.com/tcmspsearch.php) for retrieval, the search conditions were "**shudihuang** (SD)", "**shanyao** (SY)", "**shanzhuyu** (SZY)", "**fuling** (FL)", "**zhuling** (ZL)", "**zexie** (ZX)", "**haijinsha** (HJS)", "**tinglizi** (TLZ)", "**gouqizi** (GQZ)", "**sharen** (SR)" and "**danggui** (DG)", respectively. Screening conditions were set according to ADME parameters: oral bioavailability (OB) ≥30% and druglikeness (DL) ≥0.18 were considered as screening conditions. To obtain the effective components and target proteins of Jinshui Tinling decoction (JSTLD). Through Uniprot database (https://www.uniprot.org/), enter all target protein names, provided that the constraint conditions are "Popular Human" and "Reviewed" to find the gene name corresponding to a target protein with active component from a human proven protein database, With Perl 5.26.3 software (https://www.perl.org/get.html) to select target genes.

2.2. MPE related targets

Through GeneCards database (https://genealacart.genecards.org/) and OMIM database (https://www.omim.org/), the retrieval condition of "Malignant pleural effusion" was used to obtain the relevant target genes of MPE and establish the MPE gene dataset.

2.3. Construction of "drug-component-target" Network

The visual network diagram of TCM components and intersection targets was constructed using Cytoscape 3.8.2 (https://cytoscape.org/) software. The degree values of nodes were calculated by Network Analysis. Furthermore, the interaction relationship between the active components of Jingshui Tinling Decoction (JSTLD) and MPE related targets was elucidated.

2.4. Establishment of protein interaction (PPI) network

Using STRING database (https: To introduce the potential target of Jinshui-Tinling decoction (JSTLD) in the treatment of MPE, set up the species type "homo sapiens", construct the protein interaction network (PPI), and obtain the protein interaction information tsv file of the target gene. The key target genes of Jinshui Tinling decoction (JSTLD) in the treatment of MPE were obtained by count descending order.

2.5. GO function and KEGG pathway enrichment analysis

The key nodes were converted into gene ids by using the data package "org.Hs.eg.db" in R language, and then imported into R 4.0.4 software. The threshold was set $P < 0.01$. "BiocManager" and other software packages were used to analyze the GO function and KEGG enrichment of key nodes, and the biological significance and possible mechanism of MPE treatment were analyzed.

2.6. Molecular docking

The core compound of JSTLD was docked with protein, and the molecular structure of the core compound of JSTLD was downloaded from TCMSP database. The small molecules were hydrogenated and ROOT was added by AutoDock software. The RCSB (https://www.rcsb.org/) database was used to download the protein structure, and AutoDock software was used to remove water molecules and hydrogenate the protein, etc. AutoDock vina software was used to semi-flexible docking of compound molecules and proteins. Pymol software was used to render the images and output the results.

3. Results and analysis

3.1. Active ingredients and potential targets of JSTLD

TCMSP database by screening conditions (OB ≥ 30%, DL≥ 0.18), and 153 active ingredients were obtained, as shown in Table 1. There were 8,463 targets. Among them, SD, SZY and ZX share sitosterol as the active ingredient. The common active ingredient was stigmasterol in SD, SY, SZY, DG, GQZ and SR. HJS and TLZ have nemorosa kaempferol as active ingredient. GQZ and TLZ have common active ingredient quercetin. The active ingredient of DG, GQZ, TLZ, SZY, HJS and SR is β-sitosterol. After deleting the duplicate data, 128 active ingredients of JSTLD were obtained.

Table 1: Active ingredients of Jingshui Tinling Decoction

TCM	Mol ID	Molecule Name	OB (%)	DL
SD	MOL000359	sitosterol	36.91390583	0.7512
	MOL000449	Stigmasterol	43.82985158	0.75665
SY	MOL001559	piperlonguminine	30.71142726	0.1802
	MOL001736	(-)-taxifolin	60.50621692	0.27342
	MOL000310	Denudatin B	61.47237606	0.37838
	MOL000322	Kadsurenone	54.72301284	0.37829
	MOL005429	hancinol	64.0132681	0.37314
	MOL005430	hancinone C	59.04593444	0.38965
	MOL005435	24-Methylcholest-5-enyl-3belta-O-glucopyranoside_qt	37.57681789	0.71653
	MOL005438	campesterol	37.57681789	0.71488
	MOL005440	Isofucosterol	43.77639556	0.7576
	MOL000449	Stigmasterol	43.82985158	0.75665
	MOL005458	Dioscoreside C_qt	36.38228738	0.87051
	MOL000546	diosgenin	80.87792491	0.80979

	MOL005461	Doradexanthin	38.15575048	0.53662
	MOL005463	Methylcimicifugoside_qt	31.69348525	0.23655
	MOL005465	AIDS180907	45.32835933	0.77301
	MOL000953	CLR	37.87389754	0.67677
SZY	MOL001494	Mandenol	41.99620045	0.19321
	MOL001495	Ethyl linolenate	46.10096327	0.19716
	MOL001771	poriferast-5-en-3beta-ol	36.91390583	0.75034
	MOL002879	Diop	43.59332547	0.39247
	MOL002883	Ethyl oleate (NF)	32.39738821	0.19061
	MOL003137	Leucanthoside	32.11589283	0.78146
	MOL000358	beta-sitosterol	36.91390583	0.75123
	MOL000359	sitosterol	36.91390583	0.7512
	MOL000449	Stigmasterol	43.82985158	0.75665
	MOL005360	malkangunin	57.71384384	0.62642
	MOL005481	2,6,10,14,18-pentamethylicosa-2,6,10,14,18-pentaene	33.4041173	0.24028
	MOL005486	3,4-Dehydrolycopen-16-al	46.64445252	0.4906
	MOL005489	3,6-Digalloylglucose	31.41521237	0.66343
	MOL005503	Cornudentanone	39.6634055	0.327
	MOL005530	Hydroxygenkwanin	36.46699689	0.27206
	MOL005531	Telocinobufagin	69.99386894	0.79297
	MOL008457	Tetrahydroalstonine	32.41977527	0.81311
	MOL000554	gallic acid-3-O-(6'-O-galloyl)-glucoside	30.25032187	0.6746
	MOL005552	gemin D	68.8303535	0.56075
	MOL005557	lanosta-8,24-dien-3-ol,3-acetate	44.29553995	0.82425
FL	MOL000273	(2R)-2-[(3S,5R,10S,13R,14R,16R,17R)-3,16-dihydroxy-4,4,10,13,14-pentamethyl-2,3,5,6,12,15,16,17-octahydro-1H-cyclopenta [a]phenanthren-17-yl]-6-methylhept-5-enoic acid	30.93214234	0.81281
	MOL000275	trametenolic acid	38.71150002	0.80199
	MOL000276	7,9(11)-dehydropachymic acid	35.105891	0.81091
	MOL000279	Cerevisterol	37.96382825	0.77061
	MOL000280	(2R)-2-[(3S,5R,10S,13R,14R,16R,17R)-3,16-dihydroxy-4,4,10,13,14-pentamethyl-2,3,5,6,12,15,16,17-octahydro-1H-cyclopenta [a]phenanthren-17-yl]-5-isopropyl-hex-5-enoic acid	31.07205665	0.81528
	MOL000282	ergosta-7,22E-dien-3beta-ol	43.50708637	0.71939
	MOL000283	Ergosterol peroxide	40.36268048	0.81255
	MOL000285	(2R)-2-[(5R,10S,13R,14R,16R,17R)-16-hydroxy-3-keto-4,4,10,13,14-pentamethyl-1,2,5,6,12,15,16,17-octahydrocyclopenta[a]phenanthren-17-yl]-5-isopropyl-hex-5-enoic acid	38.255158	0.82014
	MOL000287	3beta-Hydroxy-24-methylene-8-lanostene-21-oic acid	38.69991401	0.8095
	MOL000289	pachymic acid	33.62791957	0.81076
	MOL000290	Poricoic acid A	30.60694619	0.76152
	MOL000291	Poricoic acid B	30.52460129	0.7463
	MOL000292	poricoic acid C	38.15135789	0.74643
	MOL000296	hederagenin	36.91390583	0.75072
	MOL000300	dehydroeburicoic acid	44.17229867	0.83458
ZL	MOL000279	Cerevisterol	37.96382825	0.77061
	MOL000282	ergosta-7,22E-dien-3beta-ol	43.50708637	0.71939
	MOL000796	(22e,24r)-ergosta-6-en-3beta,5alpha,6beta-triol	30.19604056	0.76433
	MOL000797	(22e,24r)-ergosta-7,22-dien-3-one	44.87660559	0.72485
	MOL000798	ergosta-7,22-diene-3 -ol	43.50708637	0.71913
	MOL000801	5alpha,8alpha-epidioxy-(22e,24r)-ergosta-6,22-dien-3beta-ol	44.39151838	0.82192
	MOL011169	Peroxyergosterol	44.39151838	0.82
	MOL000816	ergosta-7,22-dien-3-one	44.87660559	0.72456
	MOL000817	ergosta-5,7,22-trien-3-ol	46.18489919	0.72348
	MOL000820	polyporusterone E	45.71302909	0.85389
	MOL000822	polyporusterone G	33.43027891	0.81312
ZX	MOL000359	sitosterol	36.91390583	0.7512
	MOL000830	Alisol B	34.47307308	0.81706

	MOL000831	Alisol B monoacetate	35.57623621	0.80629
	MOL000832	alisol, b,23-acetate	32.51621601	0.81841
	MOL000849	16s -methoxyalisol B monoacetate	32.42724106	0.7679
	MOL000853	alisol B	36.76038067	0.81993
	MOL000854	alisol C	32.70016921	0.81507
	MOL000856	alisol C monoacetate	33.06358947	0.82763
	MOL002464	1-Monolinolein	37.17662836	0.30249
	MOL000862	[(1S,3R)-1-[(2R)-3,3-dimethyloxiran-2-yl]-3-[(5R,8S,9S,10S,11S,14R)-11-hydroxy-4,4,8,10,14-pentamethyl-3-oxo-1,2,5,6,7,9,11,12,15,16-decahydrocyclopenta [a]phenanthren-17-yl]butyl] acetate	35.57623621	0.80765
HJS	MOL001506	Supraene	33.54594264	0.42161
	MOL001689	acacetin	34.97357273	0.24082
	MOL001790	Linarin	39.84373106	0.70925
	MOL002879	Diop	43.59332547	0.39247
	MOL002881	Diosmetin	31.13794879	0.27442
	MOL002882	[(2R)-2,3-dihydroxypropyl] (Z)-octadec-9-enoate	34.13107758	0.29824
	MOL002883	Ethyl oleate (NF)	32.39738821	0.19061
	MOL000296	hederagenin	36.91390583	0.75072
	MOL000358	beta-sitosterol	36.91390583	0.75123
	MOL000422	kaempferol	41.88224954	0.24066
TLZ	MOL002211	11,14-eicosadienoic acid	39.99355408	0.20044
	MOL000296	hederagenin	36.91390583	0.75072
	MOL000354	isorhamnetin	49.60437705	0.306
	MOL000358	beta-sitosterol	36.91390583	0.75123
	MOL003905	K-STROPHANTHOSIDE	70.64964761	0.22162
	MOL003906	K-STROPHANTHOSIDE_qt	30.79711254	0.77587
	MOL003907	erysimoside	65.4545739	0.22876
	MOL003908	Cynotoxin	99.94245194	0.7759
	MOL003909	evobioside	44.24660976	0.24322
	MOL003927	Dihomolinolenic acid	44.11029883	0.20398
	MOL000422	kaempferol	41.88224954	0.24066
	MOL000098	quercetin	46.43334812	0.27525
GQZ	MOL001323	Sitosterol alpha1	43.28127042	0.78354
	MOL003578	Cycloartenol	38.68565906	0.78093
	MOL001494	Mandenol	41.99620045	0.19321
	MOL001495	Ethyl linolenate	46.10096327	0.19716
	MOL001979	LAN	42.11918897	0.74787
	MOL000449	Stigmasterol	43.82985158	0.75665
	MOL000358	beta-sitosterol	36.91390583	0.75123
	MOL005406	atropine	45.97058178	0.19328
	MOL005438	campesterol	37.57681789	0.71488
	MOL006209	cyanin	47.42092269	0.75918
	MOL007449	24-methylidenelophenol	44.19264545	0.7533
	MOL008173	daucosterol_qt	36.91390583	0.75316
	MOL008400	glycitein	50.47891366	0.23826
	MOL010234	delta-Carotene	31.80094312	0.54639
	MOL000953	CLR	37.87389754	0.67677
	MOL009604	14b-pregnane	34.77923299	0.33723
	MOL009612	(24R)-4alpha-Methyl-24-ethylcholesta-7,25-dien-3beta-ylacetate	46.35749925	0.8398
	MOL009615	24-Methylenecycloartan-3beta,21-diol	37.31728162	0.79751
	MOL009617	24-ethylcholest-22-enol	37.09454086	0.7511
	MOL009618	24-ethylcholesta-5,22-dienol	43.82985158	0.75636
	MOL009620	24-methyl-31-norlanost-9(11)-enol	37.9996853	0.75092
	MOL009621	24-methylenelanost-8-enol	42.36819868	0.76769
	MOL009622	Fucosterol	43.77639556	0.75668
	MOL009631	31-Norcyclolaudenol	38.68209614	0.81391
	MOL009633	31-norlanost-9(11)-enol	38.35394137	0.7249

	MOL009634	31-norlanosterol	42.20462055	0.73012
	MOL009635	4,24-methyllophenol	37.83467433	0.74999
	MOL009639	Lophenol	38.12940252	0.714
	MOL009640	4alpha,14alpha,24-trimethylcholesta-8,24-dienol	38.90988973	0.75772
	MOL009641	4alpha,24-dimethylcholesta-7,24-dienol	42.65304098	0.75297
	MOL009642	4alpha-methyl-24-ethylcholesta-7,24-dienol	42.29509453	0.78304
	MOL009644	6-Fluoroindole-7-Dehydrocholesterol	43.72602513	0.72224
	MOL009646	7-O-Methylluteolin-6-C-beta-glucoside_qt	40.77368843	0.30497
	MOL009650	Atropine	42.15897078	0.19299
	MOL009651	Cryptoxanthin monoepoxide	46.95371937	0.56103
	MOL009653	Cycloeucalenol	39.72647216	0.79446
	MOL009656	(E,E)-1-ethyl octadeca-3,13-dienoate	41.99620045	0.19364
	MOL009660	methyl (1R,4aS,7R,7aS)-4a,7-dihydroxy-7-methyl-1-[(2S,3R,4S,5S,6R)-3,4,5-trihydroxy-6-(hydroxymethyl)oxan-2-yl]oxy-1,5,6,7a-tetrahydrocyclopenta[d]pyran-4-carboxylate	39.42847682	0.46558
	MOL009662	Lantadene A	38.67942417	0.57405
	MOL009664	Physalin A	91.70647491	0.27207
	MOL009665	Physcion-8-O-beta-D-gentiobioside	43.90358656	0.62426
	MOL009677	lanost-8-en-3beta-ol	34.22630373	0.74036
	MOL009678	lanost-8-enol	34.22630373	0.74167
	MOL009681	Obtusifoliol	42.55200222	0.7565
	MOL000098	quercetin	46.43334812	0.27525
SR	MOL001755	24-Ethylcholest-4-en-3-one	36.08361164	0.75703
	MOL001771	poriferast-5-en-3beta-ol	36.91390583	0.75034
	MOL001973	Sitosteryl acetate	40.38964165	0.85102
	MOL000358	beta-sitosterol	36.91390583	0.75123
	MOL003975	icosa-11,14,17-trienoic acid methyl ester	44.81361719	0.23355
	MOL000449	Stigmasterol	43.82985158	0.75665
	MOL007180	vitamin-e	32.28642803	0.69563
	MOL007514	methyl icosa-11,14-dienoate	39.6670588	0.22908
	MOL007535	(5S,8S,9S,10R,13R,14S,17R)-17-[(1R,4R)-4-ethyl-1,5-dimethylhexyl]-10,13-dimethyl-2,4,5,7,8,9,11,12,14,15,16,17-dodecahydro-1H-cyclopenta[a]phenanthrene-3,6-dione	33.1153996	0.78802
	MOL007536	Stigmasta-5,22-dien-3-beta-yl acetate	46.44190225	0.85691
DG	MOL000358	beta-sitosterol	36.91390583	0.75123
	MOL000449	Stigmasterol	43.82985158	0.75665
SY, GQZ	MOL005438	campesterol	37.57681789	0.71488
SY, GQZ	MOL000953	CLR	37.87389754	0.67677
SZY, HJS	MOL002883	Ethyl oleate (NF)	32.39738821	0.19061
SZY, HJS	MOL002881	Diosmetin	31.13794879	0.27442
SZY, SR	MOL001771	poriferast-5-en-3beta-ol	36.91390583	0.75034
SZY, GQZ	MOL001495	Ethyl linolenate	46.10096327	0.19716
SZY, GQZ	MOL001494	Mandenol	41.99620045	0.19321
HJS, TLZ	MOL000422	kaempferol	41.88224954	0.24066
FL, ZL	MOL000282	ergosta-7,22E-dien-3beta-ol	43.50708637	0.71939
FL, ZL	MOL000279	Cerevisterol	37.96382825	0.77061
GQZ, TLZ	MOL000098	quercetin	46.43334812	0.27525
SD, SZY, ZX	MOL000359	sitosterol	36.91390583	0.7512
FL, HJS, TLZ	MOL000296	hederagenin	36.91390583	0.75072
SD, SY, SZY, DG, GQZ, SR	MOL000449	Stigmasterol	43.82985158	0.75665
DG, GQZ, TLZ, SZY, HJS, SR	MOL000358	beta-sitosterol	36.91390583	0.75123

3.2. Targets of JSTLD components and MPE disease targets

JSTLD was retrieved through TCMSP database, and 195 target sites were obtained after all component targets were combined and removed. 1539 relevant target sites of "Malignant pleural

effusion" were retrieved using GeneCards database and OMIM database, and the intersections were obtained. 106 common targets were obtained, as shown in Figure 1. The potential target genes of Jinshui Tinling decoction in the treatment of MPE are shown in Table 2.

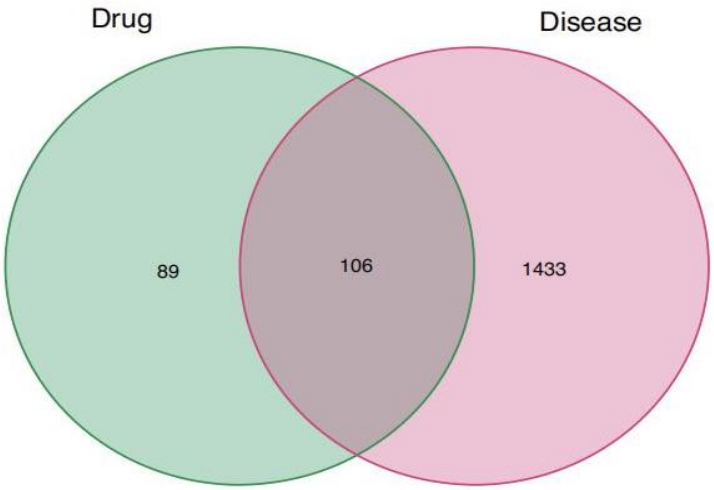

Figure 1: Venn diagram of active component targets and MPE related targets in Jingshui Tinling Decoction

Table 2: Potential targets of Jinshui Tinling decoction in the treatment of MPE

The name of the gene						
PGR	PLAU	TOP2A	TP53	ICAM1	ALOX5	RASSF1
PTGS1	LTA4H	DPP4	NFKBIA	IL1B	IL1A	E2F1
PTGS2	MAOB	F2	TOP1	CCL2	MPO	ACP3
HSP90AA1	LYZ	MMP3	SOD1	SELE	ABCG2	CTSD
ADRB2	DRD2	RELA	MMP1	VCAM1	NFE2L2	IGFBP3
BCL2	ESR1	EGFR	HIF1A	CXCL8	PARP1	IGF2
BAX	PPARG	AKT1	STAT1	PRKCB	COL3A1	CD40LG
CASP9	GSK3B	CCND1	CDK1	BIRC5	CXCL11	IRF1
JUN	CDK2	BCL2L1	HSPA5	HSPB1	CXCL2	ERBB3
CASP3	CHEK1	FOS	ERBB2	IL2RA	CHEK2	RASA1
CASP8	PRSS1	CDKN1A	HMOX1	NR1I2	CLDN4	GSTM1
PRKCA	CCNA2	MMP2	CYP3A4	PLAT	PPARA	FASLG
PON1	NOS2	MMP9	CAV1	THBD	PPARD	CYP19A1
NR3C2	MMP8	MAPK1	MYC	SERPINE1	CXCL10	SLPI
RXRA	NR3C1	IL6R	F3	IFNG	SPP1	ABCC2
MTOR						

3.3. "Drug-ingredient-target" network

Cytoscape 3.8.2 software was used to draw the "drug-component-target" network diagram of Jinshui Tinling decoction (JSTLD) in the treatment of MPE, as shown in Figure 2. The network consists of 201 nodes. The top 4 active ingredients were quercetin, β-sitosterol, kaempferol and stigmasterol according to the node parameter degree values, which were 188, 78, 66 and 54, respectively.

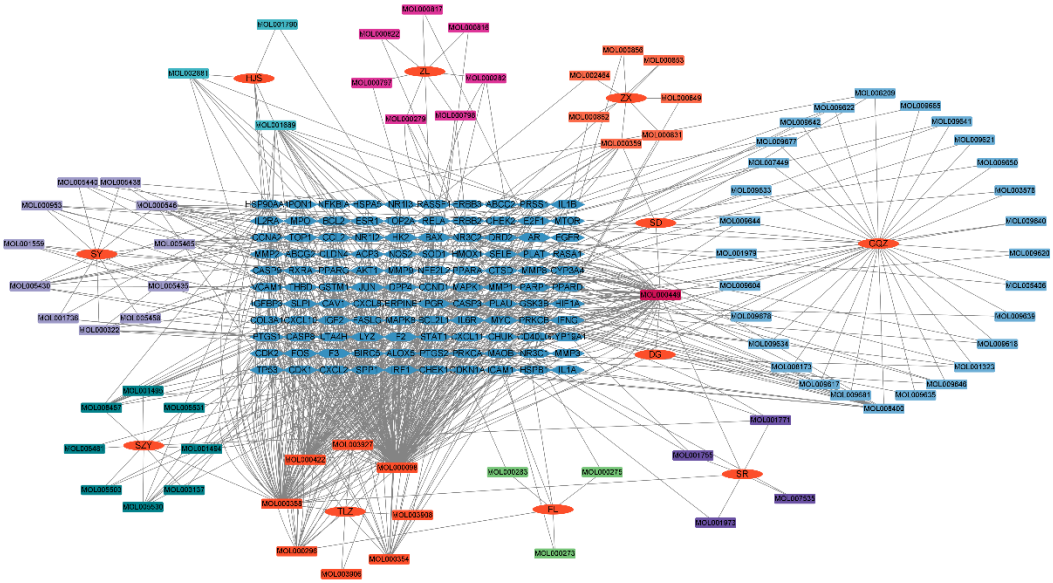

Figure 2: Drug-component-target network diagram of Jinshui Tinling decoction in the treatment of MPE

Note: ovals represent drugs; The rectangle represents the active ingredient; The hexagon represents the target

3.4. PPI network

With the help of STRING database, the species "homo sapiens" was set for 106 intersection targets to draw PPI network, as shown in Figure 3. The top 30 key targets were analyzed in descending order of count value. As shown in figure 4. The results showed that AKT1, TP53, IL1B, CASP3, JUN, EGFR, MMP9, MYC, HIF1A, CXCL8 and other genes may be the key target genes of JSTLD in the treatment of MPE.

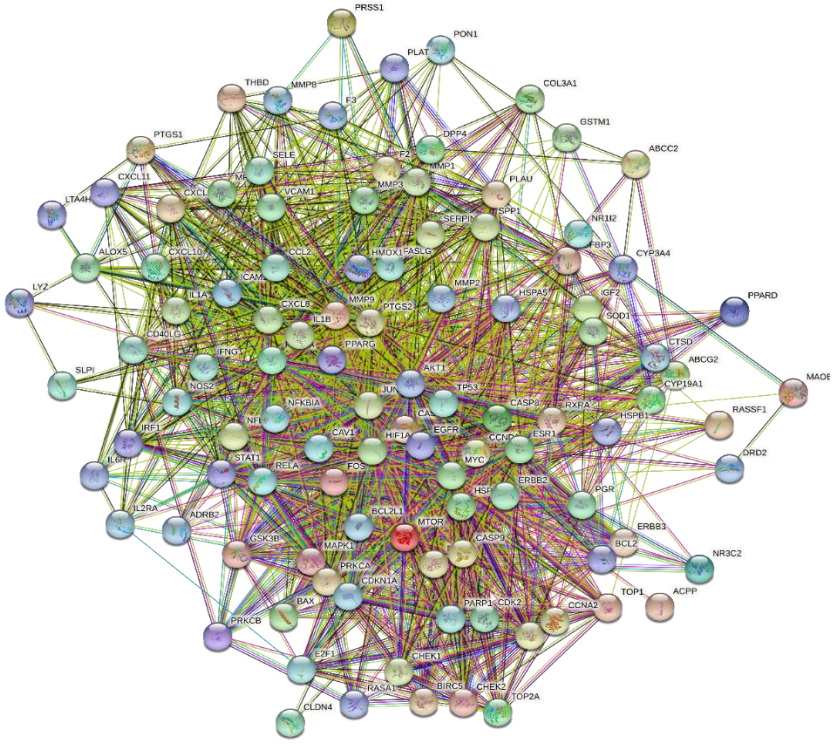

Figure 3: PPI network diagram of Jinshui Tinling decoction for MPE targets

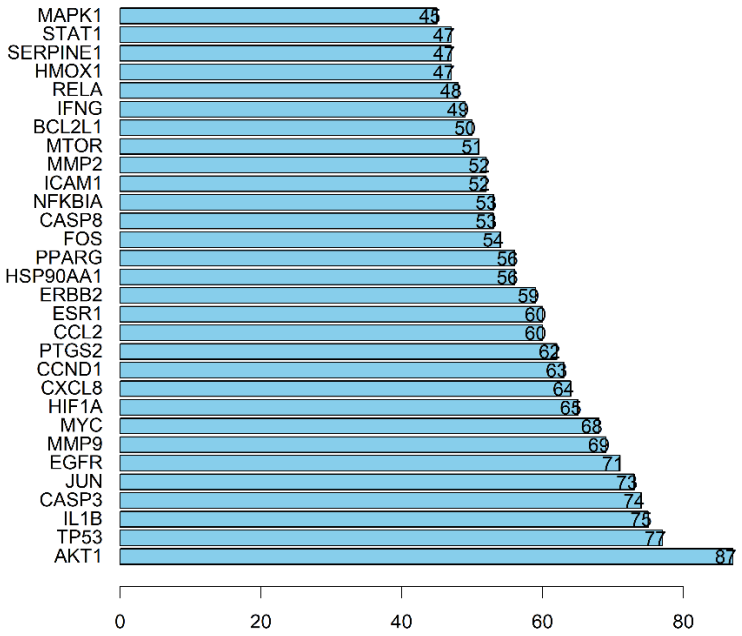

Figure 4: Key Targets (Top 30)

3.5. GO function and KEGG pathway enrichment analysis

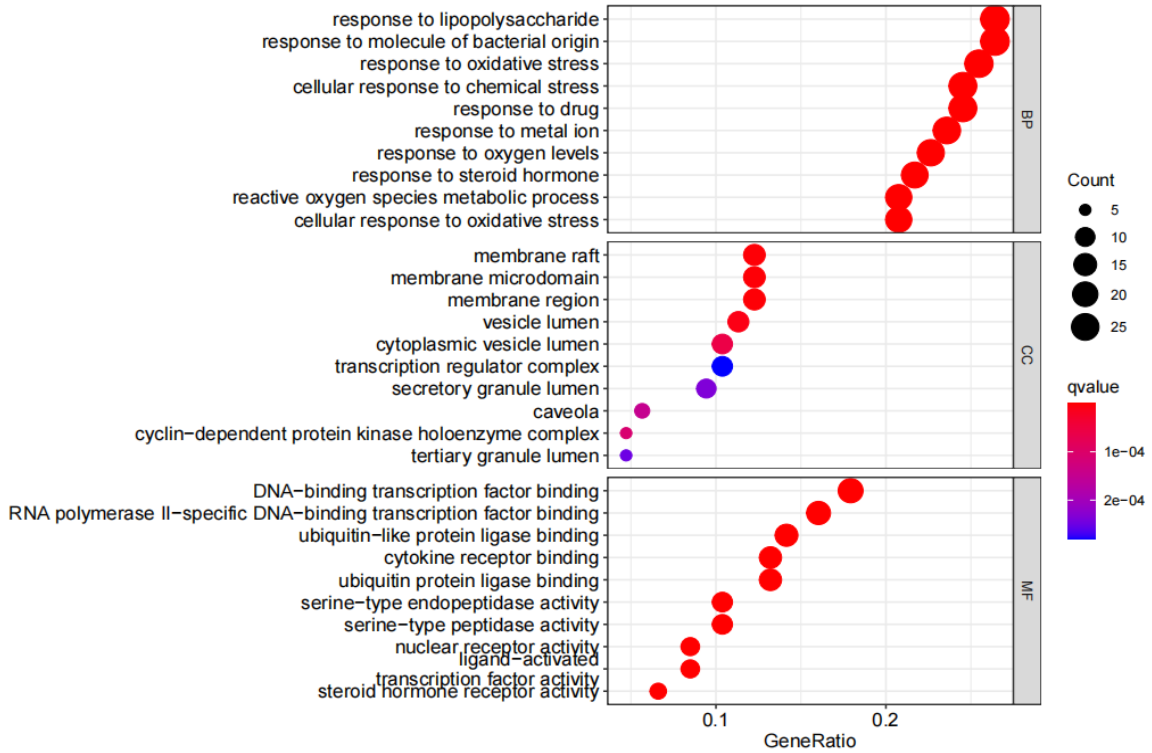

Figure 5: GO functional analysis results (Top 10)

GO functional analysis results showed that Biological Processes (BP) included 4,367 data, mainly focusing on the reaction to lipopolysaccharide, the reaction to bacterial-derived molecules, the reaction of cells to oxidative stress and other biological processes. CC, Cellular Components, a total of 399 data, mainly concentrated in membrane raft, membrane microzone, membrane zone, etc. A

total of 140 Molecular Functions were collected, mainly focusing on DNA-binding transcription factor binding, RNA polymerase II-specific DNA-binding transcription factor binding, ubiquitin like protein ligase binding, etc. As shown in figure 5. KEGG pathway enrichment analysis results showed 233 signaling pathways including cancer pathway, HIF-1 signaling pathway, NF-kappa B signaling pathway, JAK-STAT signaling pathway, etc. P value represents the degree of enrichment, and the most significant degree of enrichment is cancer pathway, as shown in Figure 6.

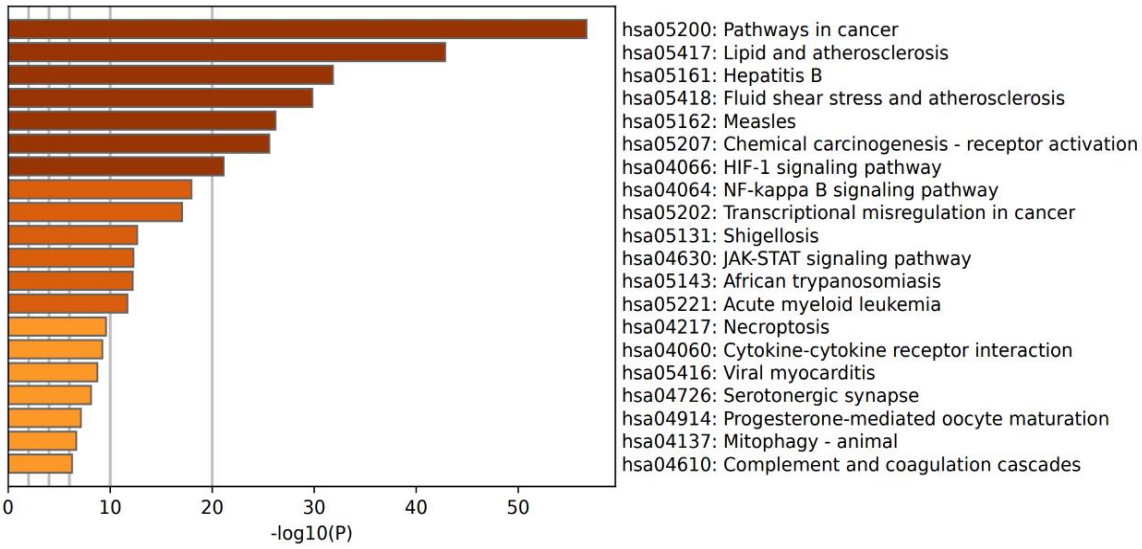

Figure 6: KEGG pathway enrichment analysis results (Top 20)

3.6. Molecular docking results

The top 10 targets with PPI degree value and the top 4 pharmacodynamic components with "drug-ingredient-target" network graph degree value were respectively used to establish molecular docking models, and the docking scores were shown in Table 3. Autodock vina 1.1.2 software was used to select key targets of protein interaction and their compounds for molecular docking. The results of molecular docking showed that the lowest binding energy of the top 4 active components and the top 10 key target receptors with the degree of PPI were less than -5 kcal/mol, and they were closely bound with strong binding activity, as shown in Figure 7.

Table 3: Molecular docking information between key compounds and core target proteins

Target	Stigmasterol	kaempferol	quercetin	beta-sitosterol
AKT1	-9.3	-7	-9.2	-9.8*
TP53	-8.4*	-7.5	-6.3	-8.3
IL1B	-6.8	-6.3	-6.1	-6.5
CASP3	-8.2*	-7.5	-7.5	-7.3
JUN	-8.4	-9*	-8.7	-7.8
EGFR	-8.3*	-7.6	-7.7	-7.8
MMP9	-8.5*	-7	-7.1	-7.7
MYC	-8.8*	-7.4	-7	-8.1
HIF1A	-6.2	-6.6	-6.2	-6.7*
CXCL8	-6.8*	-5.6	-5.1	-6.5

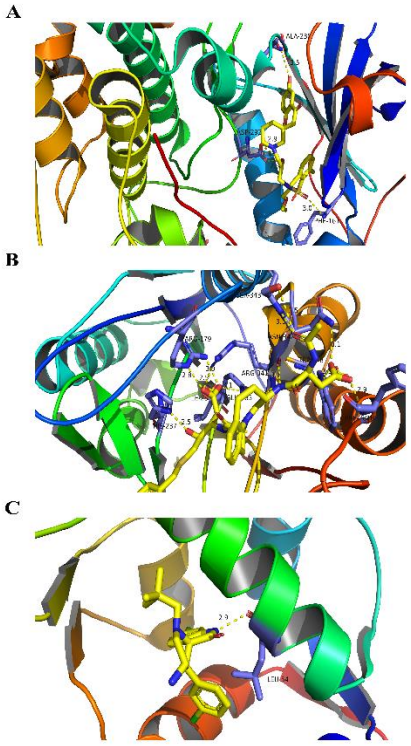

A: beta-sitosterol&AKT1; B: Stigmasterol&TP53; C: Stigmasterol&CASP3

Figure 7: Docking pattern diagram of therapeutic components and target of Jinshui Tinling decoction

4. Conclusions and Discussion

In this study, quercetin, β-sitosterol, kaempferol and stigmasterol were selected as the main active ingredients of JSTLD. Relevant studies have shown that quercetin and other EGFR small molecule inhibitors [8-9]. Studies have shown that silver nanoparticles mediated by β-sitosterol in human colon cancer HT-29 cells exhibit cytotoxic effects, which can accelerate the apoptosis of colon cancer cells and have various pharmacological effects such as cancer inhibition, anti-inflammatory and anti-apoptosis [10-12]. Kaempferol is a flavonoid extracted from rhizoma kaempferiae kaempferiae. It can destroy the nucleus of cancer cells by synthesizing K-AuNCs, induce apoptosis and autophagy, inhibit the proliferation of A549 cells and treat lung cancer. Studies have shown that kaempferol has anti-cancer, antibacterial, anti-inflammatory and other effects [13-17]. Stigmasterol can reduce the transcription of tumor necrosis factor-α, destroy tumor angiogenesis, inhibit the growth of cholangiocarcinoma, and reduce the proliferation and migration of gastric cancer cells by inhibiting JAK/STAT signaling pathway [18].

The results of PPI network analysis showed that AKT1, TP53, IL1B, CASP3, JUN and EGFR were the core targets of JSTLD in the treatment of MPE. In the process of tumor occurrence and development, AKT1 is a key factor for PI3K to inhibit apoptosis and plays an important role through PI3K/Akt/mTOR signaling pathway [19-20]. Studies have found that TP53 mutation promotes the proliferation, migration and invasion of tumor cells [21]. Il-1β plays an important role in immune defense and immune-mediated diseases [22]. Tumorigenesis is related to the release of inflammatory mediators, pyroptosis, multiple signaling pathways and resistance to chemotherapy drugs [23]. In the process of gastric cancer chemotherapy, the cell mortality of SGC-7901 and MKN-45 was significantly increased after fluorouracil treatment, indicating that pyroptosis of gastric cancer cells

is caused by caspase-3-dependent apoptosis induced by chemotherapy drugs [24]. These findings suggest that caspase-3 activation can induce necrosis mediated by cleavage of the Gasdermin E family, providing new insights into tumor chemotherapy [25-26]. Cellular inflammatory response is closely related to the activation of JNK/c-Jun signaling pathway [27]. The mutation of upstream EGFR and PIK3CA often leads to the mutation and overactivation of AKT, which promotes the further deterioration of lung cancer [28].

The main pathogenesis of MPE is the increase of pleural permeability caused by pleural tumors (malignant tumor metastasis, mesothelioma) and the obstruction of parietal pleural lymphatic drainage caused by lymphatic obstruction of cancer. As the most important signaling pathway in the treatment of MPE by JSTLD, cancer pathway may play an important role in the treatment of MPE.

In summary, the results of this study showed that quercetin, β-sitosterol, kaempferol and stigmasterol were the key components of JSTLD. Core target proteins AKT1, TP53, IL1B, CASP3, JUN, EGFR and other targets; Cancer pathway is the most important signal pathway in the treatment of MPE with JSTLD. The minimum binding energy of all the molecular docking results was less than -5.0 kJ ·mol-1, indicating good docking, which further indicated the rationality of JSTLD in the treatment of MPE. JSTLD plays an important potential role in inhibiting the proliferation of cancer cells, which has certain guiding significance for further research. However, this study also has some shortcomings. Experimental verification of active ingredients, core targets and key signaling pathways is needed in the future to verify the mechanism of action of JSTLD in the treatment of MPE.

Acknowledgements

Natural Science Foundation of Shaanxi Province (2021JM-565): Jinshui-Tingling Decoction inhibits the formation and mechanism of malignant pleural effusion in mice; Shaanxi University of Traditional Chinese Medicine Postgraduate Academic Exchange Program (XSJL005): To investigate the mechanism of Jinshui-Tingling decoction in the treatment of malignant pleural effusion of non-small cell lung cancer based on network pharmacology and in vitro Western Blot experiments

The First Author: Baogang Yang, (1990-), male, master student of Shaanxi University of Traditional Chinese Medicine. Research direction: Integrated traditional Chinese and Western medicine clinical tumor. Email: youaremysmile153@163.com

Second author and corresponding autho: Chenguang Yang*, (1971-), male, doctoral candidate, chief physician, master tutor of Shaanxi University of Traditional Chinese Medicine, Shaanxi Hospital of Traditional Chinese Medicine. Research direction: Integrated traditional Chinese and Western medicine clinical tumor. Email: 470999091@qq.com

Third author: Jiao Gou, (1988-), female, Shaanxi Provincial Hospital of Traditional Chinese Medicine, postgraduate, associate chief physician. Research direction: Integrated traditional Chinese and Western medicine clinical tumor. Email: sunnyxjdt@qq.com

References

[1] Fitzgerald Db, Koegelenberg C, Yasufuku K, Et al. Surgical and non-surgical management of malignant pleural effusions [J]. Expert Rev Respir Med, 2018, 12(1): 15 to 26.

[2] Feller-Kopman DJ, Reddy CB, DeCamp MM, et al. Management of Malignant Pleural Effusions. An Official ATS/STS/STR Clinical Practice Guideline. Am J Respir Crit Care Med. 2018; 198 (7): 839-849.

[3] Bibby AC, Dorn P, Psallidas I, et al. ERS/EACTS statement on the management of malignant pleural effusions. Eur Respir J. 2018; 52(1): 1800349. Published 2018 Jul 27.

[4] Recuero Diaz JL, Figueroa Almanzar S, Galvez Munoz C, et al. Recommendations of the Spanish Society of Thoracic Surgery for the management of malignant pleural effusion. Cir Esp (Engl Ed). 2022 Jun 3: S2173-5077(22)00160-0.

[5] Yang Chenguang, Wang Songhai, Xu Peng. Treatment of malignant pleural effusion from the perspective of water and fire in mingmen [J]. Shaanxi journal of traditional Chinese medicine, 2019, 40(2): 247-249.

[6] Yang C G. A kind of Chinese medicine composition used in the treatment of malignant pleural effusion [P]. China

Invention Patent, CN111939239B. 2022-02-01.
[7] Kang Chao, Yang Baogang, Yang Chenguang, et al. A retrospective analysis of Mingmen theory in the treatment of malignant pleural effusion [J]. Clinical Medical Research & Practice. 2022(13): 94-97.
[8] Yu Q, Fan L, Duan Z. Five individual polyphenols as tyrosi- nase inhibitors: inhibitory activity, synergistic effect, action mechanism and molecular docking [J]. Food Chem, 2019, 297: 124910.
[9] Salaverry L S, Parrado A C, Mangone F M, et al. In vitro anti-inflammatory properties of Smilax campestris desalination extract in human macrophages. characterization of full its flavo- noid profile [J]. J Ethnopharmacol, 2020, 247: 112-282.
[10] Shathviha PC, Ezhilarasan D, Rajeshkumar S, et al. β-sitosterol mediated silver nanoparticles induce cyto- toxicity in human colon cancer HT-29 cells [J]. Avi- cenna J Med Biotechnol, 2021,13 (1): 42-46.
[11] Luna-Herrera C, Intranigral administration of β-sitosterol-β-D-glucoside elicits neurotoxic A1, MARTINEZ DAVILA LA, SOTOROJASLO, et al. Intranigral administration of β-Sitosterol-β-D-glucoside Elicits Neurotoxic A1 astrocyte reactivity and chronic neuroinflammation in the rat substantia nigra [J]. J Immunol Res, 2020 (712): 1-19.
[12] Chen Y , Chen J , Sun K , et al. To Explore the Mechanism of Dahuang Fuzi Xixin Decoction in Treatment of Renal Interstitial Fibrosis Based on Network Pharmacology[J]. Journal of Liaoning University of Traditional Chinese Medicine, 2020.
[13] Wang H J, Chen L Y, Zhang X Y, Et Al. Kaempferol protects mice from d-GalN/LPS-induced acute liver failure by regulating the ER stress-Grp78-CHOP signaling pathway [J]. Biomed Pharmacoth, 2019, 111(12): 468-475.
[14] Han X, Liu C F, Gao N, et al. Kaempferol suppresses proliferation but increases apoptosis and autophagy by up-regulating microRNA-340 in human lung cancer cells [J]. Biomed Pharmacoth, 2018, 108: 809-816.
[15] Zhong X M, Zhang L, Li Y M, Et Al., Kaempferol alleviates ox - LDL - induced apoptosis by the up - regulation of miR - a - 5 p 26 via inhibiting TLR4 / the nf-kappa B pathway in human endothelial cells [J]. Biomed Pharmacoth, 2018, 108(17): 1783-1789.
[16] Govindaraju Saravanan, Roshini Arivazhagan, Lee Min-Ho, et al. Conjugated gold nanoclusters enabled efficient for anticancer Ther-apeutics to A549 lung cancer cell [J]. International journal of nanomedi-cine, 2019, 14: 5147-5157.
[17] Xue Han, Chun-Fang Liu, Na Gao, et al. Kaempferol suppresses proliff-eration but, Macrophages and autophagy by up-regulating microRNA-340 in human lung Cancer cells [J]. Journal of Biomedicine & amp; Pharmacotherapy, 2018, 108: 809-816.
[18] Wang Shuai, Sun Yu, Li Chunmei, Lu Qun. Research progress of stigmasterol [J]. China Pharmaceutical, 2019, 28(23): 96-98.
[19] Zughaibi Ta, Suhail M, Tarique M, Et al. Targeting PI3K/Akt/mTOR pathway by different flavonoids: [J]. Int J Mol Sci, 2019, 22 (22): 12455. (In Chinese)
[20] Sun E J, Wankell M, Palamuthusingam P, et al. Tar- geting the PI3K/Akt/mTOR pathway in hepatocellular carcinoma [J]. Biomedicines, 2021, 9 (11): 1639.
[21] Yan Jiali, Li Hui. Effect of TP53 and EGFR co-mutation on the prognosis of NSCLC patients after first-line TKI treatment [J]. Inner Mongolia Medical Journal, 2020, 52(1): 23-27.
[22] Mantovani A, Dinarello C A, Molgora M, et al. Interleukin-1 and related cytokines in the regulation of inflammation and immunity [J]. Immunity, 2019, 50(4): 778-795.
[23] ZHOU CB, gastrointestinal cancer and immune responses to intestinal microbial infection [J]. Gastrointestinal Cancer, Gastrointestinal and intestinal microbial Infection chimica et Biophysica Acta Reviews on Cancer, 2019, 1872 (1): 1-10.
[24] Wang Y, Yin B, Li D, Et al. GSDME mediates caspase-3-de-pendent pyroptosis in gastric cancer [J]. Biochemical and Bio-physical Research Communications, 2018,495 (1): 1418-1425.
[25] Wang Y, Gao W, Shi X, Et al. Erythrodrugs induce py-roptosis through caspase-3 cleavage of a gasdermin [J]. Nature, 2017,547 (7661): 99-103.
[26] Jiang Mx, Qi L, Li Ls, Et al. apoptosis in apoptosis induced by apoptosis in vitro [J]. Cell Death Discov, 2020,6 (12): 112-122.
[27] Yan B, Peng Z, Xing X, et al. Glibenclamide induces apoptosis by activating reactive oxygen species dependent JNK pathway in hepato- cellular Carcinoma cells [J]. Bioscience Reports, 2017; 37 (5): BSR20170685.
[28] Tan, A C. Targeting the PI3K/Akt/mTOR pathway in non-small cell lung cancer (NSCLC) [J]. Thorac Cancer, 2020, 11 (3): 511-518.